pH Dependence of the Crystal Violet Adsorption Isotherm at the Silica−Water Interface

Jonathan D. Fisk, Robin Batten, Glenn Jones, Josephine P. O'Reilly, and Andrew M. Shaw*

School of Biological and Chemical Sciences, University of Exeter, Stocker Road, Exeter EX4 4QD, UK

Received: March 9, 2005; In Final Form: May 25, 2005

The pH-dependent adsorption isotherms for the charged chromophore crystal violet, CV^+, have been measured with three different bases by a free-running cavity implementation of evanescent wave cavity ring-down spectroscopy. The ratio of the maximal absorbance measurements at pH 5.10 and 9.05 is consistent with a Q2:Q3 silanol site ratio of 72.8:27.2. The adsorption isotherms have been interpreted in terms a cooperative binding adsorption allowing more than one ionic species to bind to each silanol group. The surface concentration is consistent with a silanol charge density of 1.92 ± 0.55 nm^{-2} and a total neutralized interface layer structure extending 9 nm from the surface. Binding constants and stoichiometric coefficients are derived for CV^+ to both the Q2 and Q3 sites. A variation of the adsorption isotherm with base is observed so that the isotherm at pH 9.05 adjusted with ammonium hydroxide sets up a competitive acid−base equilibrium with the SiOH groups with only 49% of the surface silanol sites dissociated. The implications for functionalized surfaces in chromatography are discussed.

Introduction

The adsorption of charged species at the silica−water interface is an important process in understanding the environmental sinks, both terrestrial and aquatic, of a number of pesticides and heavy metal ions. Theories of cooperative binding have been developed for binding to humic matter[1] culminating in a thermodynamically consistent isotherm known as the NICCA-Donnan binding model.[2,3] The theory has been applied widely in the interpretation of biofilm formation at the silica−water interface[4] and the binding of Gram positive bacteria[5] stimulating adhesive proteins (adhesins) production.

NMR studies[6] reveal the silica surface contains two types of silanol group: SiOH known as Q2 and Q3 both with different pK_a values. The Q2 site has two Si−OH groups pointing away from the surface with two Si−O groups pointing into the bulk, $(O_2-Si)-(OH)_2$, whereas the Q3 site has the structure $(O_3Si)-OH$, Figure 1. Cooperative binding of a charged species to the Q3 group can be written as follows:

$$(O_3Si)-O^- + nI^+ \rightarrow (O_3Si)-O^-I_n^+ \qquad (1)$$

where n is the stoichiometric binding coefficient, which need not be an integer, and I^+ is a counterion. The binding of a large charged species to rough surfaces in particular must be cooperative, recognizing that the binding of a single ion does not neutralize each charged site on the surface exactly in a one-to-one adsorption isotherm. Partial neutralization of the surface sites due to steric reasons allows for additional cooperative binding of a second or multiple species to the residual charge, Figure 1. The bilayer formed in the interface will contain both positive counterions and some negative co-ions from the bulk brought into the layer with the incoming counterions. The surface can also undergo polarity reversal binding a positive dication such as Ca^{2+} to the Q3 site switching the surface charge from negative to positive.

* Address correspondence to this author. E-mail: andrew.m.shaw@exeter.ac.uk.

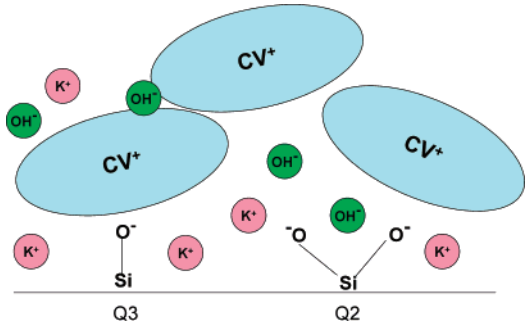

Figure 1. Cooperative binding to the Q3 and Q2 silanol sites.

Interpretation of n requires an understanding of the nature of cooperative binding and was first introduced in the binding of oxygen to haemoglobin (Hb) in the form of the Hill equation,[7] where Hill plots revealed the binding of 4 O_2 groups to the Hb protein. The binding stoichiometry is also noninteger when derived from humic acids binding studies. This is interpreted as an effective soil binding in terms of affinity distributions[8] of binding sites although this too will depend on the binding geometry of the counterion. In this paper, we extend the concept of cooperative binding stoichiometry to the neutralization of the silica−water interface by monitoring the binding of the charged chromophore crystal violet (CV^+) to the silanol groups at two different bulk pH values and hence surface potential.

The direct measurement of optical absorbance at the silica surface requires an ultra sensitive adsorption spectroscopic technique such as evanescent wave cavity ring-down spectroscopy (e-CRDS). Cavity ring-down spectroscopy (CRDS) has proven to be an important technique for the detection of small numbers of molecules in the gas phase[9,10] by direct absorption. Recently, CRDS has been extended to samples in bulk liquids.[11,12] It is also possible to use CRDS to detect absorption by species at interfaces using an attenuated total reflection (ATR) configuration, notably the adsorption of I_2 to the silica surface by Pipino.[13] Other studies have looked at the charged properties of the silica−water interface including the titration

10.1021/jp051211z CCC: $30.25
Published on Web 07/13/2005

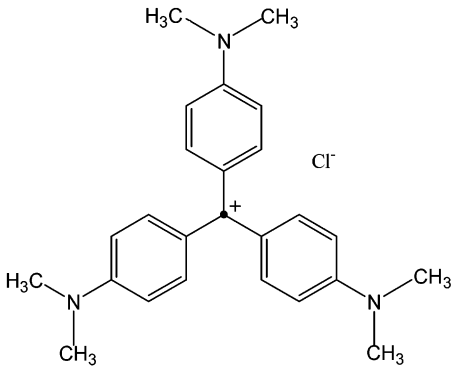

Figure 2. Structure of crystal violet.

of the SiOH groups[14] and group density. Measurements have also been made of the adsorption isotherm of Hb binding to form a protein biofilm.[4]

The structure of charged interfaces is conventionally understood in terms of the Gouy−Chapman−Stern mean-field theory of charged electrode interfaces,[15] but no consideration is given to the nature of the binding within the Stern or the other sublayers, such as the inner and outer Helmholtz plane. The silica−water interface has been studied previously by a number of techniques including nonlinear optics,[16,17] ATR with thermal lens detection,[18] and fluorescence microscopy.[19] In addition, the silica surface has been studied by cross-polarization magic angle spinning NMR[6] revealing the presence of two different surface ^{19}Si signals having a negative chemical shift, δ, with respect to the solution TMS standard. This observation is consistent with the second harmonic generation (SHG) studies by Eisenthal et al.[16] which suggest the silica surface contains two types of titratable silanol groups. Group 1 constitutes 19% of the surface silanol sites and has a pK_a(1) of 4.5; group 2 comprises the remaining 81% of the surface sites and has a pK_a(2) of 8.5. A study by Dong, Pappu, and Xu[17] reported a silanol group density of 8.2×10^{13} cm^{-2} or 0.8 groups nm^{-2}, although estimates[20] have varied with the largest at 8 groups nm^{-2}.

The adsorption of a charged crystal violet counterion (CV^+), Figure 2, to the silica−water interface should show a significant pH dependence that varies with the site density and the relative proportions of the Q2 and Q3 sites. The adsorption isotherm for CV^+ has been measured at a low pH of 5.10 where the binding will be dominated by the deprotonated Q3 site and at pH 9.05 where Q2 binding will prevail. A cooperative binding isotherm model has been developed to interpret the data and the implications for the structure of the charged silica−water interface are discussed.

Experimental Methods

The direct observation of molecules bound to the surface requires an absorbance sensitivity beyond that available with conventional spectrometers. However, the free-running Dove cavity e-CRDS implementation has enabled an absorbance sensitivity of 6×10^{-6}, 6 ppm, to be observed under normal conditions.

A stable, linear optical resonator of length 0.85 m is formed from two high reflectivity mirrors (99.95% Layertech), one with a radius of curvature of 1 m and the other planar. Light from a continuous wave broad band laser (5 mW, wavelength 635 nm) is introduced to the cavity through the back of the flat mirror from a fiber-optic coupled collimator with a spot size of 1 mm at a focal length of 1 m. Laser radiation fills the cavity due to the overlap between the bandwidth of the laser and several cavity modes. The intrinsic narrow laser line width required for the measurement of rotationally resolved gas-phase spectra requires the laser to be locked to one of the cavity modes. These locked-cavity cw measurements have provided some of the most sensitive gas-phase direct absorbance measurements with sensitivities to within a factor of 50 of the shot-noise limit. Measurement of absorbance in the solution phase does not require the same intrinsic wavelength resolution as the absorption features of optical spectra may be several hundreds of nanometers wider.

The diode laser is centered at 635 nm with a bandwidth of ±2 nm and overlaps several longitudinal modes of the Dove cavity. The wavelength of the cavity modes is given by:

$$\lambda = \frac{2l}{n} \tag{2}$$

where n is the mode number, λ is the wavelength of the mode, and l is the length of the cavity. From eq 2, the laser overlaps some 1.7×10^4 longitudinal cavity modes and so is always in resonance and light always enters the cavity. The laser is no longer locked to just one mode and may be said to be a free-running configuration of e-CRDS.

The radiation from the laser is allowed to build up in the cavity to an intensity level determined by the Q-factor of the cavity with a ring-up time, τ, determined by the mirror reflectivity. The laser radiation is then interrupted and the radiation rings down with the same decay time, τ. The present free-running configuration interrupts the laser power supply at 6 kHz allowing a rapid data collection rate. The data are averaged over 256 traces on a digital oscilloscope (Lecroy, 1Gs) and transferred to a PC. A nonlinear Levenberg−Marquart routine is used to fit the data to a single-exponential functional form to derive the ring-down time, τ. An average of four estimates of τ is made to determine a mean, μ, and standard deviation, σ, from which $\sigma\tau/\tau$ can be determined. The ring-down time τ is formally the ring-down time of 1.7×10^4 different cavity modes, each with a slightly different τ determined by the variation in the bandwidth of the mirror reflectivity. Assuming this is constant over for the number of modes overlapped by the laser, the practical variation limit of $\sigma\tau/\tau$ is ~0.01% or 100 ppm, which is close to the 8-bit resolution limit of the digital oscilloscope.

A Dove prism (Sigma Optics, UK) was introduced into the cavity equidistant from the mirrors with a p-polarized antireflection coating (SLS Optics, UK) centered at 635 nm with a minimum reflection of ~0.5% giving an empty cavity ring-down time τ of 450 ns and an ultimate absorbance sensitivity of 1.5×10^{-6}, 1.5 ppm (typically 5 ppm). The Dove prism configuration preserves the path of the radiation within the cavity and introduces a total internal reflection (TIR) event at the back surface of the prism. TIR results in the generation of an evanescent wave at the prism reflecting surface with an electric field that decays exponentially into the medium above. The characteristic penetration depth, d_p, is determined by:

$$d_p = \frac{\lambda}{2\pi((\sin(\vartheta))^2 - {n_{12}}^2)^{1/2}} \tag{3}$$

where λ is the wavelength of the radiation propagating in the prism, θ is the angle of incidence at the interface with respect to the normal, and n_{12} is the ratio of the refractive index of the prism (1.4677 at 635 nm) to the medium above the prism. For the current configuration, with water, the penetration depth is 189.2 nm. The beam waist at the center of the cavity explores

a projected circular path on the back surface of the prism with an area of 0.41 mm^2.

A single-pass flow cell was constructed from polytetrafluoroethene (PTFE) with a flow channel matched to the prism width of 10 mm machined into the underside of the block. Once clamped and sealed to the upper prism surface with a 1 mm thick nitrile "O"-ring, the flow cell volume was 190 μL. Samples were allowed to flow through the cell with a maximum flow rate of 4 mL per hour from a syringe pump; this corresponded to a maximum linear flow velocity of 0.14 mm s^{-1}. The velocity of the flow through the cell determines the rate of transfer of molecules from the bulk solution to the surface. Calculation of the flow Reynolds Number indicates the type of flow regime present within the cell. This is found from:

$$\{\mathrm{Re}\} = \frac{\rho u d}{\mu} \tag{4}$$

where ρ is the fluid density, u is the flow velocity, d is the characteristic flow dimension, and μ is the fluid viscosity. Assuming fluid viscosity and density to be equal to that of water at 25 °C (i.e., 0.8909 $\times$ 10^{-3} N s m^{-2} and 998 kg m^{-3}, respectively) with a cell dimension of 1 mm, the Reynolds Number is 0.16. With highly viscous, laminar flow in ducts existing up to Reynolds Numbers exceeding 1, this value indicates that the flow regime within the cell was truly laminar and thus diffusion limiting conditions prevailed. At such slow flows, the laminar boundary layer is estimated to be fully developed within 1 μm of the cell entrance. Therefore, the electrostatic attraction of the CV^+ to the silica surface will dominate.

Crystal violet (Acros Organics, high purity) was used without further purification and made up into solution with ultrapure water (18 MΩ cm^{-1}) in the range 0.05−200 μM. The prism surface cleaning protocol was as follows: 1% sodium dodecyl sulfate (SDS, Sigma-Aldrich) in methanol, water, 0.1 M hydrochloric acid (HCl), saturated sodium hydroxide (NaOH), 0.1 M HCl, water, and methanol. Ultrapure water was then passed over the prism before commencing each isotherm run. The pH of the CV^+ solutions was adjusted to pH 5.10 with HCl or pH 9.05 as required, using ammonium hydroxide (NH_4OH), potassium hydroxide (KOH), or NaOH (all chemicals from Fisher Scientific) for each experiment. Ultrapure water (with pH adjusted to 5.10 or 9.05) was passed over the prism before introduction of the lowest concentration CV^+ solution. Adsorption to the silica surface occurred until equilibrium was reached and this was taken as the limiting adsorption value. The subsequent concentrations of CV^+ were introduced to the flow cell allowing the layer structure at the interface to build up cumulatively. This was repeated until the highest concentration was reached in each experiment. Several full concentration range experiments were accomplished for each type of pH adjustment of CV^+. Repeat experiments were also carried out at low CV^+ concentrations (up to 5 μM) with smaller concentration increments (0.1 μM.)

Results

Adsorption isotherms were recorded for CV^+ to the silica−water interface at two different pH values chosen to produce similar degrees of dissociation of the Q3 and Q2 SiOH groups. The ionic strength of the resulting solutions was similar but not the same. The low pH isotherm will be solely due to binding to the Q3 sites whereas the high pH isotherm will be determined by the entire silanol group population on the surface. Higher pH solutions were not chosen because CV^+ precipitates at pH values above 10−11. Three bases were chosen with similar ionic radii to investigate the competitive binding between CV^+ and Na^+, K^+ and NH_4^+ and the potential for partial surface neutralization by the ammonium ion due to proton-transfer reactions.

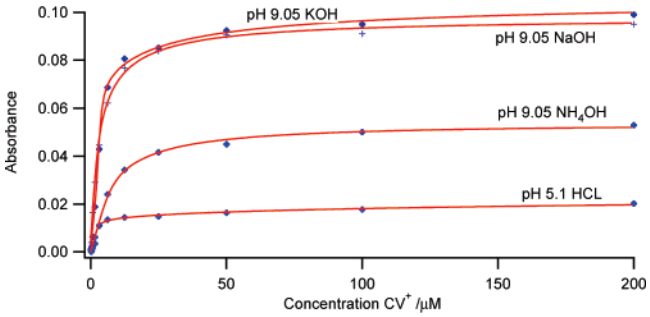

Figure 3. Adsorption isotherm for CV^+ at pH 9.05 and 5.10 for HCl, NaOH, KOH, and NH_4OH.

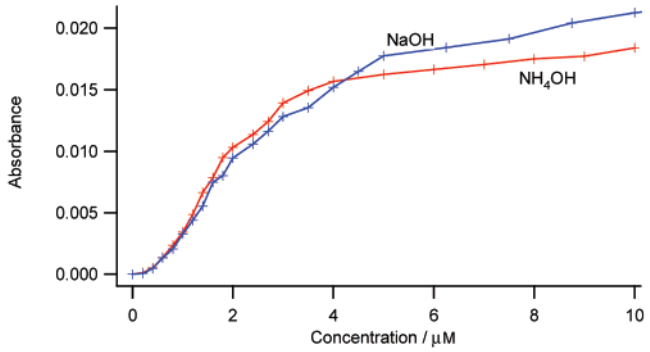

Figure 4. Low-concentration CV^+ adsorption isotherms at pH 9.05 for NH_4OH and NaOH.

Chromophore molecules present within the beam-waist footprint of the radiation within the cavity in the evanescent field will absorb laser radiation and thus remove energy from the evanescent field. Absorption from the evanescent field constitutes an additional loss in the cavity and reduces the ring-down time, τ. The change in τ can be used to calculate the absorbance due to the molecules and is given by:

$$\mathrm{Abs} = \frac{\Delta\tau}{\tau_0 \tau}\left(\frac{t_r}{2}\right) \tag{5}$$

where τ_0 is the ring-down time for the empty cavity, $\Delta\tau$ is the change in τ due to the molecular absorbance, and t_r is the round-trip time of the cavity including the propagation of the radiation through the prism material. The result is then converted to base 10 logarithms for comparison with the Beer's law expression for absorbance, Abs = ϵcl, where ϵ is the molar extinction coefficient ($M^{-1}cm^{-1}$), c is the concentration, (M), and l is the path length (cm). The time scales within the experiment are calibrated very accurately within the digital oscilloscope and hence the absorbance values are absolute. The adsorption isotherms for all three bases are shown in Figure 3 with the low-concentration isotherms shown at pH 9.05 for NaOH and NH_4OH, Figure 4. The high pH isotherm shows a significant deviation at chromophore concentrations of 1 μM not seen in the low pH isotherm and this has been well characterized.

Discussion

The adsorption isotherms at the two different pH values 5.10 and 9.05 approach a maximum adsorption that may be associated with the balancing of the total negative charge of the underlying

TABLE 1: Fitting Parameters and Constants for the Multilayer Cooperative Binding Model

	HCl isotherm value ($\mu \pm \sigma$)	NaOH isotherm value ($\mu \pm \sigma$)	KOH isotherm value ($\mu \pm \sigma$)	NH_4OH isotherm value ($\mu \pm \sigma$)
fitting parameters				
concn of the monolayer, C_m/M	17.61 ± 5.41	16.13 ± 2.42	13.16 ± 1.31	7.63 ± 0.08
binding constant, CV^+ to Q3/M^{-1}	19.847 ± 7.13	fixed	fixed	fixed
first layer Q3 stoichiometry	2.725 ± 0.582	fixed	fixed	fixed
binding constant of CV^+ to Q2/M^{-1}	0 (fixed)	$(1.6 \pm 6) \times 10^{-3}$	0.424 ± 0.385	0.117 ± 0.011
first layer Q2 stoichiometry	0 (fixed)	1.80 ± 6.34	4.901 ± 0.723	4.217 ± 0.416
binding constant, CV^+ multiplayer /M^{-1}	0.084 ± 0.037	0.243 ± 0.025	0.175 ± 0.026	0.059 ± 0.011
multilayer stoichiometry	0.341 ± 0.024	1.107 ± 0.115	0.994 ± 0.133	1.002 ± 0.108
ratio of Q2:Q3 72.8:27.2	fixed	fixed	fixed	fixed
fitting constants				
refractive index prism at 635 nm	1.4677			
excitation wavelength/nm	635			
ϵ(635 nm)/M^{-1} cm^{-1} (pH 5.10 and 9.05 measured in solution)	6712	6164	6164	6164
incident angle/deg	72.8			

silica surface. The charge of the silica surface depends on the pK_a values of the underlying Q2 and Q3 sites and the degree of dissociation at the bulk pH. Defining the dissociation constant for each group, K_{Qi}, the degree of dissociation is given by:

$$K_{Qi} = \frac{[SiO^-][H_3O^+]}{[SiOH - SiO^-]} = [H_3O^+]\frac{\alpha}{(1-\alpha)} \quad (6)$$

where α is the degree of dissociation. Taking the values of $pK_{Q3} = 4.5$ and $pK_{Q2} = 8.5$, the degree of dissociation for each Q3 is 79.9% at pH 5.1 and that for Q2 is 78.6% at pH 9.05. Thus the degree of dissociation is similar for each group. The maximum absorbance for each isotherm can be converted to a concentration by using the solution phase extinction coefficients at the two bulk pH values, Table 1, from which the Q2:Q3 site ratio may be determined as 72.8:27.2. This is in excellent agreement with value of 80:20 derived from SHG measurements and determinations of the pK_a values for each site in the same study.[16]

The absorbance of the components within the charge-layered interface is the convolution of the concentration profile with the electric field of the evanescent wave:

$$\text{Abs} = \epsilon \int_0^\infty c(z) \exp(-z/d_p)\, dz \quad (7)$$

where $c(z)$ is the concentration profile normal to the surface, z is the normal, d_p is the penetration depth of the evanescent field, and ϵ is the extinction coefficient for CV^+ at the bulk pH. The extinction coefficient is assumed to have the same value as determined in solution from the UV/vis spectrum. The absorbance is then formally the Laplace transform of the concentration profile.

The low-concentration adsorption isotherm shown in Figure 4 is a detailed variation of the binding indicating immediately that a simple Langmuir adsorption isotherm model is not appropriate and that cooperative binding to the surface occurs for low chromophore densities. It is also clear from Figure 4 that the reproducibility of the surface requires careful cleaning to maintain a consistent site density although the surface is not completely neutralized by the bound layer until the bulk concentration is in excess of 100 μM. A cooperative binding model has been constructed for the concentration profile of the charged layer. The profile is divided into 1 nm sections from the surface with the first layer binding to the silica surface directly. Direct binding to the Q2 and Q3 sites is controlled by two different binding constants and a stoichiometric coefficient with the surface coverage given by:

$$\vartheta_1 = \frac{(K_1[CV^+])^{n1}}{1 + (K_1[CV^+])^{n1}}$$

$$\vartheta_2 = \frac{(K_2[CV^+])^{n2}}{1 + (K_2[CV^+])^{n2}}$$

$$C_0 = (\vartheta_1 n1 r + (1-r)\vartheta_2 n2) C_m \quad (8)$$

where θ_1 is the surface coverage, Q3 sites have a binding constant K_1 and stoichiometric coefficient $n1$, and, θ_2, K_2, and $n2$ refer to the Q2 site. C_m is the maximum concentration in the first layer and C_0 is the fractional volume; C_0/C_m is the fractional layer occupancy. The relative ratio, r, of the two species Q2:Q3 is fixed at the absorbance maximum values of 72.3:27.7.

All subsequent layers have expressions for layer coverage of the form:

$$\vartheta_l = \frac{(K_l[CV^+])^{nl}}{1 + (K_l[CV^+])^{nl}}$$

$$C_l = \vartheta_l nl C_m \quad (9)$$

where the binding to subsequent layers has a binding constant and stoichiometric coefficient different for the binding to silica surface layer but the same for all subsequent layers into the interface.

The parameters of the model may be constrained by the properties of the silica surface already present in the literature from a number of sources but principally the SHG measurements.[16] The concentration of positively charged species next to the negatively charged surface depends on the surface charge density. The Grahame equation[15] relates the surface concentration of species to the surface charge density:

$$\rho_0 = \frac{\sigma^2}{2\epsilon_r \epsilon_0 kT} \quad (10)$$

where σ is the surface charge density (C m^{-2}), ϵ_r is the relative permittivity of water (74.89), ϵ_0 is the permittivity of free space, k is the Boltzmann constant, and T is the temperature. Typical site densities are $1-2$ nm^{-2}, which corresponds to a surface concentration of 7.5−29.9 M: C_m was restricted between these

values within the fit. The number of layers was then increased until the calculated final absorbance was close to the observed value, setting the number of 1 nm layers at 9. This was held fixed throughout the fit.

The parameters in the binding model were fitted to the experimental data for the isotherm at pH 5.10 assuming binding only to the Q3 site and negligible binding to the Q2 site. The concentration profile was constructed by using the cooperative binding model and transformed numerically. The model parameters were fitted to the experimental data by using a Levenberg−Marquart nonlinear least-squares fitting routine with results presented in Table 1. All parameters associated with Q2 binding were set to zero for the low pH isotherm, allowing Q3 binding and subsequent layers to be optimized. Fitting to the pH 9.05 adsorption isotherm was achieved by fixing the binding constants for the Q3 binding sites and allowing the parameters for the Q2 sites and multilayer binding constants to float. The results of the fitting are also presented in Table 1.

The fitted value of C_m for the pH 5.10 isotherm is 17.6 ± 5 M corresponding to a surface site density of 1.5 ± 0.8 nm^{-2} which, when corrected for the 79.9% dissociation of the Q3 site, gives a site density on the surface of 1.92 ± 0.55 nm^{-2}, in excellent agreement with other reported values.[16] The C_m parameter is also sensitive to competitive biding between the CV^+ chromophore and the cation of the base. V_m shows a decreasing trend from the predominantly Q3-dissoicated surface with HCl, being smaller for NaOH and KOH. The increasing surface charge should decrease the volume of the first layer next to the surface with the chromophore being held nearer the surface by the Coulombic interactions. However, effective competitive binding with Na^+ ions excludes the chromophore from the surface requiring a larger C_m to model the total absorbance. K^+ is less competitive with the chromophore and more CV^+ ions approach and bind to the surface requiring a smaller C_m to model the total absorbance.

The isotherm for the weak base NH_4OH shows a considerably smaller C_m and final total absorbance indicating a new equilibrium is set up between the Q2 SiOH group with a pK_a of 8.5 and the NH_4^+ ion. The equilibria of interest are:

$$\mathrm{SiOH} + \mathrm{OH^-} \leftrightarrow \mathrm{SiO^-} + \mathrm{H_2O} \qquad (K_{Q2})$$

$$\mathrm{NH_4^+} + \mathrm{SiO^-} \leftrightarrow \mathrm{SiOH} + \mathrm{NH_3} \qquad (K_3)$$

$$\mathrm{NH_4^+} + \mathrm{OH^-} \leftrightarrow \mathrm{NH_3} + \mathrm{H_2O} \qquad (K_4) \qquad (11)$$

Rearranging the equations and eliminating the NH_3 gives the equilibrium constant K_3 in terms of K_4 and the degree of dissociation of the surface:

$$K_3 = \frac{K_4[\mathrm{OH^-}]}{\vartheta} \qquad (12)$$

Estimating θ either from the ratio of the ultimate absorbances for NaOH and NH_4OH or the ratio of the V_m parameters for the HCl and NH_4OH isotherms gives a value for $\theta = 0.49$; assuming p$K_4 = 4.73$, an estimate of p$K_3 = 9.35$ can be made. This is an important observation indicating that despite a high pH only about 49% of the SiOH groups are dissociated and negatively charged.

The nature of the multilayered interface is usually understood in terms of the conventional models of Gouy−Chapman (GC) or Stern−Gouy−Chapman (SGC) detailed elsewhere.[15] The dimensions of the interface in a diffuse layer model depend on the Debye length and hence the ionic strength of the solution. The ionic strength of the solutions in our investigations is low in the bulk, corresponding to a Debye length for a diffuse layer of ∼97 nm for the solutions at both pH 5.10 and 9.05 falling to 21 nm at 200 μM CV^+. The cooperative binding model, however, neutralizes the surface completely within 9 layers of adsorption corresponding to an interface layer thickness of ∼9 nm. Direct binding to the silica surface appears to form a layer, perhaps the Stern layer, which completely neutralizes the surface, restricting the charged interface to only a few nanometes for charged species.

The ionic strength of the solution within the layer is, however, much higher than in the bulk with surface concentrations of order 17 M. The high ionic strength is also asymmetric between positive and negative ions in the interface with a Boltzmann enhanced counterion population at the fully charged surface. This is some 2 orders of magnitude larger than in the bulk, whereas the co-ion (solution phase negative ions entering the interface with the counterions) concentration is depleted by a similar amount. The concentrations of the ionic species within the layer must correctly be described by the activities of the ionic species and it is also unlikely that the relative permittivity of the layer is fixed at the weak-dilute solution value of 74.89. It is also clear from the good agreement with the literature values that the extinction coefficient of the chromophore does not change markedly at the interface compared with the bulk value. The insulating silica surface is unlikely to polarize the molecule and the charged chromophores will not π-stack efficiently without a neutralizing co-ion layer, the concentration of which is depleted in the interface. The formation of dye aggregates is unlikely.

The fitted values of the stoichiometric coefficients for the Q3 binding suggest that within the 1 nm near-surface layer there are 2.7 CV^+ molecules consistent with the cooperative binding represented schematically in Figure 1. The Q2 binding coefficient for NaOH is much smaller at 1.8 consistent with effective competitive binding with the Na^+ and the silanol group. The fit to the NaOH data is less confident with the Q2 binding showing considerable uncertainty in the determined parameters. Competitive binding between the larger K^+ cation and the chromophore does not interfere with either NH_4^+ or K^+ as these have well-determined stoichiometric coefficients, ∼4.5, in the near-surface layer. The multilayer stoichiometry is rather small at pH 5.10 for low surface potentials but is closer to 1 for all of the higher layers.

The measured stoichiometric coefficients and binding constants compare favorably with reported values in the literature for the distribution of charge centers on complex humic materials such as soils.[8,21] Multilayer formation is well-established for even the simplest metal ions when binding to the silica−water interface. The previous measurements[14] with CV^+ as the chromophore, using e-CRDS, assumed a Langmuir adsorption isotherm to the silica surface and derived a model for the surface acidity. This model and the titration data can now be refined in terms of the multilayer structure by using the cooperative binding NICCA-Donnan model. This will be readily extended to interpret the titration data in the presence of the multiply charged cations Ca^{2+} and La^{3+}, changing the charge on the surface from negative through the point of zero charge to positive.

The low concentration regions of the isotherm for both bases NaOH and NH_4OH show a point of inflection at a bulk concentration of 2 μm and 1.8 μM, respectively. The surface concentration for these bulk concentrations with the fully

dissociated surface is 200 and 180 μM and must correspond to a phase transition in the structure of the initial bilayer. The surface concentration is still 2 orders of magnitude smaller than the concentration of the first layer. The transition in the structure of the bilayer appears to be related to an increase in the volume with a concomitant reduction in the surface concentration. The model presented in eqs 8 and 9 does not provide a description of the observed behavior.

Conclusions

A cooperative binding model has been developed to interpret the adsorption isotherm for a charged chromophore at the silica−water interface. The chromophore isotherm is pH sensitive and dependent on the degree of surface charge. The fundamental surface properties derived from this study are consistent with the accepted values. e-CRDS measurements provide new insight into the structure and composition of the charged interface structure and the role of the base in activating the surface. Chromatography experiments requiring basic solutions and different surface functionalization can control the degree of surface charge at the silica−water interface, influencing or moderating retention times. The role of amines in raising the pH and controlling the surface charge can be exploited in preparing the chromatography surfaces.

Acknowledgment. The authors would like to thank the EPSRC for funding this research.

References and Notes

(1) Koopal, L. K.; van Riemsdijk, W. H.; Kinniburgh, D. G. *Pure Appl. Chem.* **2001**, *73*, 2005.

(2) Kinniburgh, D. G.; van Riemsdijk, W. H.; Koopal, L. K.; Borkovec, M.; Benedetti, M. F.; Avena, M. J. *Colloids Surf., A* **1999**, *151*, 147.

(3) Christensen, J. B.; Tipping, E.; Kinniburgh, D. G.; Grøn, C.; Christensen, T. H. *Environ. Sci. Technol.* **1998**, *32*, 3346.

(4) Martin, W. B.; Mirov, S.; Marydtk, D.; Shaw, A. M. *J. Biomed. Opt.* Accepted for publicaiton, 2004.

(5) Plette, A. C. C.; van Riemsdijk, W. H.; Benedetti, M. F.; van der Wal, A. J. *J. Colloid Interface Sci.* **1995**, *173*, 354.

(6) Maciel, C. E. In *The Encyclopedia of Nuclear Magnetic Resonance*; Grant, D. M., Harris, R. K., Eds.; Wiley: Chichester, UK, 1996; p 4370.

(7) Van Volde, K. E. *Physical Biochemistry*, 2nd ed.; Prentice Hall, Englewood Cliffs, NJ, 1985; Chapter 3.

(8) Rusch, U.; Borkovec, M.; Daicic, J.; van Riemsdijk, W. H. *J. Colloid Interface Sci.* **1997**, *191*, 247.

(9) Berden, G.; Peeters, R.; Meijer, G. *Int. Rev. Phys. Chem.* **2000**, *19*, 565.

(10) Spence, T. G.; Harb, C. C.; Paldus, B. A.; Zare, R. N.; Willke, B.; Byer, R. L. *Rev. Sci. Instrum.* **2000**, *71*, 347.

(11) Hallock, A. J.; Berman, E. S. F.; Zare, R. N. *Anal. Chem.* **2002**, *74*, 1741.

(12) Xu, S.; Sha, G.; Xie, J. *Rev. Sci. Instrum.* **2002**, *73*, 255.

(13) Pipino, A. C. R.; Hudgens, J. W.; Huie, R. E. *Chem. Phys. Lett*. **1997**, *280*, 104.

(14) Shaw, A. M.; Hannon, T. E.; Li, F.; Zare, R. N. *J. Phys. Chem. B* **2003**, *107*, 7070.

(15) Bard, A. J.; Faulkner, L. R. *Electrochemical Methods*: *Fundamentals and Applications*, 2nd ed.; Wiley & Sons: New York, 2001.

(16) Ong, S.; Zhao, X.; Eisenthal, K. B. *Chem. Phys. Lett*. **1992**, *191*, 327.

(17) Dong, Y.; Pappu, S. V.; Xu, Z. *Anal. Chem.* **1998**, *70*, 4730.

(18) Shimosaka, T.; Sugii, T.; Hobo, T.; Ross, J. B. A.; Uchiyama, K. *Anal. Chem.* **2000**, *72*, 3532.

(19) Wirth, M. J.; Ludes, M. D.; Swinton, D. J. *Anal. Chem.* **1999**, *71*, 3911.

(20) Cox, G. B. *J. Chromatogr. A* **1993**, *656*, 353.

(21) Rytwo, G. *Appl. Clay Sci.* **2004**, *24*, 137.